ORIGINAL PAPER

Application of Optical-fiber Photoreactor for CO_2 Photocatalytic Reduction

Jeffrey C. S. Wu · Tzu-Hua Wu · Taichi Chu ·
Hungji Huang · Dingping Tsai

Abstract An optical-fiber photoreactor, comprised of 216 xcatalyst-coated fibers, was designed and assembled to transmit and spread light uniformly inside the reactor. The power loss of light transmission inside an optical fiber was calculated using beam propagation method. The optimum length of optical fiber was estimated to be near 11 cm long in order to entirely spread out light energy over surface catalyst. Vapor-phase CO_2 was photocatalytically reduced to methanol using the photoreactor under UV irradiation in a steady-state flow system. The solutions of metal-loaded titania were prepared by thermal hydrolysis method. Metal-loaded TiO_2 film was coated on optical fibers by dip-coating method. TiO_2, Cu/TiO_2 and Ag/TiO_2 films were uniformly on the fibers and their thicknesses ranged from 27 to 33 nm. The films consisted of very fine spherical particles with diameters of 10–20 nm. The XRD spectra indicated anatase phase for all films. Methanol yield increased with UV irradiative intensity. Maximum methanol rate was 4.12 μmole/g-cat h using 1.0 wt%-Ag/TiO_2 catalyst at 1.13 bar of CO_2, 0.03 bar of H_2O pressures, and 5,000 s mean residence time under 10 W/cm^2 UV irradiation.

Keywords Photocatalysis · Optical-fiber photoreactor · CO_2 conversion · Renewable energy

J. C. S. Wu (✉) · T.-H. Wu
Department of Chemical Engineering, National Taiwan
University, Taipei 10617, Taiwan, ROC
e-mail: cswu@ntu.edu.tw

T. Chu · H. Huang · D. Tsai
Department of Physics, National Taiwan University,
Taipei 10617, Taiwan, ROC

1 Introduction

Almost industrial chemical reactions are thermal-driven processes currently. The required thermal energy is mostly supplied by fossil fuel which, in fact, stored the solar energy in prehistoric times. Photocatalysis provides an alternative route to carry out reactions using photo energy, which may be directly supplied from the sun. The photonitration and photonitrosation of phenol were reported using TiO_2 catalyst under UV irradiation [1]. Photocycloadditions provided elegant routes to synthesize aromatic compounds from non-aromatics. Compared to the normal intramolecular arene–alkene, photocyclization improved the efficiency of such reactions [2]. Hydrogen will be a major energy source once the fuel cell is operated commercially. Photo-driven water splitting can generate hydrogen from solar energy without producing CO_2 [3–6].

In the last 20 years, photocatalysis has been shown to be effective for removing trace levels of persistent and toxic organic pollutants from both water and air. The photocatalyst and photo kinetics have been studied for years. However, most applications are still in the environmental remediation. Now, it is time to develop a photoreactor to extend more application in chemical processes. The major barrier for commercial applications is its high cost as well as its low overall rate and energy efficiency. This is due, among other factors, to this low-order dependency of reaction rates on radiation intensity and a limited capacity to deliver photons and reactants to catalyst surfaces. How to evenly distribute just enough photons to the catalyst surface is an crucial design factor in a photoreactor.

Our motivation is to seek photo-driven or photo-assisted chemical reactions using solar energy directly. The ideal is to use highly focused light to accelerate a photo reaction, so that mass production of chemicals is viable. The light

can be collected from the sun using focus reflection dish. TiO$_2$-coated fiber-optical cable reactors have demonstrated some inherent advantages over packed-bed reactors in photo reactions [7, 8]. Optical fibers are used to spread the light uniformly inside the module of the photoreactor. This kind of design provides an economical way to deliver photons uniformly in a large volume.
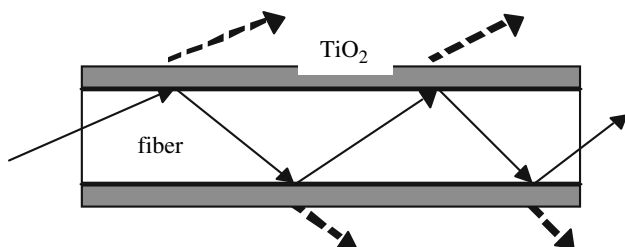
One of the most environmentally benign method to reduce greenhouse gas, CO$_2$, is the photosynthesis by plants. Green plant utilizes the solar energy to carry out photosynthesis, then converts into biomass to support all lives on the Earth. The transformation of CO$_2$ into hydrocarbons provides a direct route to produce renewable energy [9]. CO$_2$ can be photocatalytically reduced in water vapor by photocatalysts such as TiO$_2$ [10–13]. Equation 1 is an example of overall photo reduction transforming CO$_2$ to methanol. This study demonstrates a design of metal-loaded TiO$_2$ coated optical-fiber photoreactor which exhibits a good photocatalytic activity for converting CO$_2$ to methanol, as a renewable energy.

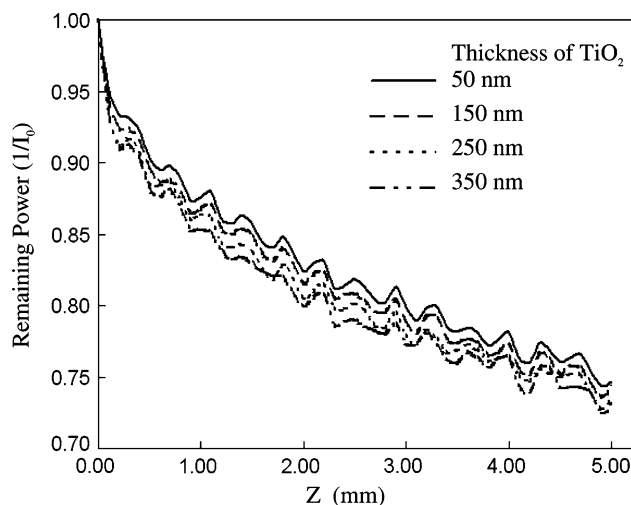$$CO_2 + 2H_2O \xrightarrow{h\nu} CH_3OH + \frac{3}{2}O_2 \qquad (1)$$
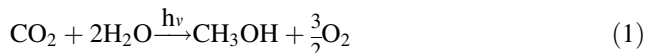
2 Theoretical Light Transmission in an Optical-fiber

Figure 1 shows that light is transmitted into an optical fiber. The light is split to two beams when hitting the internal surface of fiber, due to the difference of refraction index between the TiO$_2$ film and the quartz core. Part of the light is reflected and transmitted along the fiber, while the rest penetrates and excites the titania layer at the interface. The light gradually spreads and diminishes to the end of the fiber.

Beam propagation method (BPM) is used to calculate the transmission loss on an optical fiber [14]. Figure 2 shows the power loss in a 5 mm long TiO$_2$-coated optical fiber. The transmission loss only slightly increases with increasing TiO$_2$ thickness from 50 to 350 nm. The power loss is due to the photo energy absorbed by TiO$_2$ film, which decays exponentially along the optical fiber. Based on this result, it is estimated the remaining power decrease


Fig. 2 The remaining photo energy in an optical fiber along the transmission length (Z), light wavelength 365 nm

to 1% in a 11.4 cm long optical fiber. Thus the length of optical fiber is determined to be 11 cm so that all photo energy can be transmitted and absorbed by the surface TiO$_2$ film in a photoreactor.

3 Experimental

An optical-fiber photoreactor (OFPR) was designed and assembled to transmit light to the fiber-supported TiO$_2$ film from one side of the OFPR module, as shown in Fig. 3. Totally 216 fibers with near 11 cm long were inserted into the OFPR. The optical fibers were supported on circular plates with a diameter of 5.0 cm. The OFPR was irradiated through the quartz window of one side by a UV light source of 365 nm using EXFO, Acticure 4000. The light intensity entering the quartz window could be tuned from 1 to 16 W/cm^2. The whole OFPR was wrapped using aluminum foil to avoid the interference of indoor lamps during the reaction.

Fig. 1 The schematic of light transmission and spread of a TiO$_2$ coated-optical fiber
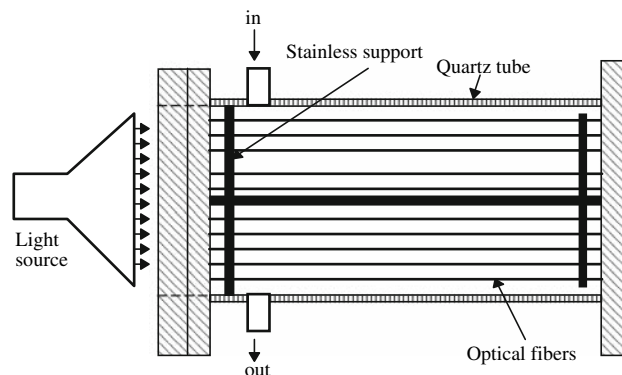
Fig. 3 Schematics of optical-fiber photo reactor

The TiO_2 solutions for coating on optical fibers were prepared using a thermal hydrolysis method. Titanium butoxide (97%, Aldrich, USA) and polyethylene glycol (PEG, molecular weight of 20,000, Merck, Darmstadt, Germany) were added to a 0.1 M nitric acid solution. An appropriate amount of metal precursor, i.e. $CuCl_2$ or $AgNO_3$, was added to obtain near 1 wt% metal loading of TiO_2. The mixed solution was stirred and heated to 80 °C for 8 h. PEG was added to prevent cracking during the drying and calcination of the film. Detailed preparation procedure was reported in literature [10].

Optical fibers were obtained from the E-Tone Technology Company of Taiwan. The polymeric shield on the optical fiber was burned off in a furnace at 400 °C. The remaining quartz fiber had a diameter of 112 μm. Each quartz fiber was cleaned by a 5 M NaOH solution in an ultrasonic cleaner, then rinsed in de-ionized water and dried before applying dip-coating procedure. The bare fiber was immersed into the solution vertically, then pulled up at a rate of 30 mm/min. The TiO_2 film was dried in air at 150 °C by a rate of 1 °C/min from the ambient temperature, and maintained at 150 °C for 3 h. Then it was calcined at 500 °C for another 5 h. The same procedure of TiO_2 coatings was also applied to glass plates for characterization.

The TiO_2 phase of the film was determined using the X-ray diffractometer, MAC Science M03XHF. The UV–visible absorption was measured by transmission mode using a Varian Cary spectrophotometer 100. The microstructure of the TiO_2 film on the optical fiber was inspected using a scanning electro microscope (SEM) LEO 1530 (Germany).

Figure 4 schematically illustrates the reactor system. Supercritical-fluid grade CO_2 was purchased from Air Products (USA) to avoid any hydrocarbon contamination. It was certified that the maximum amount of hydrocarbons was less than 20 ppb. CO_2 was bubbled through a water saturator to carry moisture. The reactor was tightly closed and maintained at 75 °C by heating tape during

the reaction. The reactor was purged for 1 h using helium before switching to CO_2. The flow rate of CO_2 was adjusted to equivalent residence time 5,000 s based on the reactor volume. The pressure of CO_2 was maintained at 1.19 bar. The saturated water pressure was 0.03 bar by adjusting the temperature of saturator. Before reaction data was taken at steady state, the fresh metal-loaded TiO_2 fibers were UV irradiated in the OFPR under CO_2 flow for 11 h to remove environmental contamination.

Reaction products were analyzed via a sampling loop of 2.5 mL on-line by a GC equipped with FID using a 2 m long Porapak Q column. Methanol, formic acid and methyl formate were detected. The Quantitative analysis indicated that methanol was the dominant hydrocarbon. The amounts of formic acid and methyl formate were much smaller than that of methanol. Methane was reported to be one of the products in the photoreduction of CO_2 on the titanium oxide prepared within the zeolite cavities [11]. But we did not detect methane due to the technique difficult of the GC analysis. Blank reactions were carried out to ensure that hydrocarbon production was solely from the photo reduction of CO_2. One blank was UV-irradiated with bare optical fibers, and another was in the dark with TiO_2-loaded optical fibers under the same experimental conditions. No hydrocarbon was detected in the above blank tests.

4 Results and Discussion

4.1 Characteristics of TiO_2 Film

Figure 5 shows the SEM cross-sections of TiO_2, Cu/TiO_2 and Ag/TiO_2 films on top of the fibers. The TiO_2, Cu/TiO_2 and Ag/TiO_2 films are uniform and their thicknesses are 31, 27 and 33 nm, respectively, on the surface of optical fiber. The films are transparent, colorless and uniformly flat without cracks. Figure 5 also shows that the all films consisted of very fine close-packed particles with diameters of 10–20 nm.
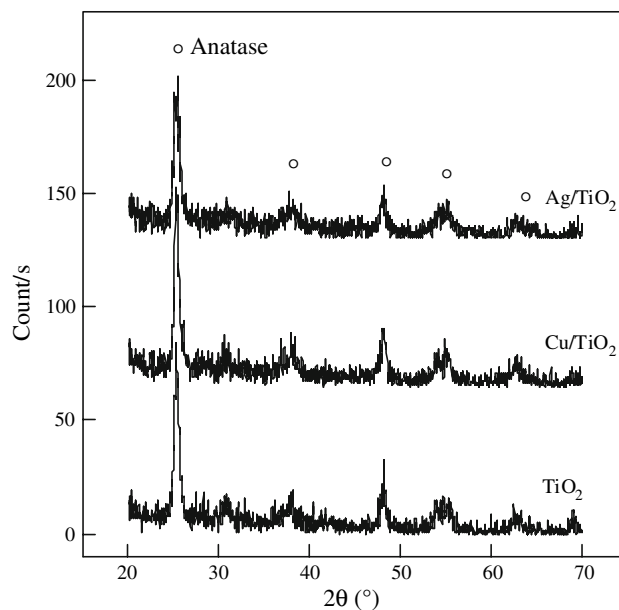
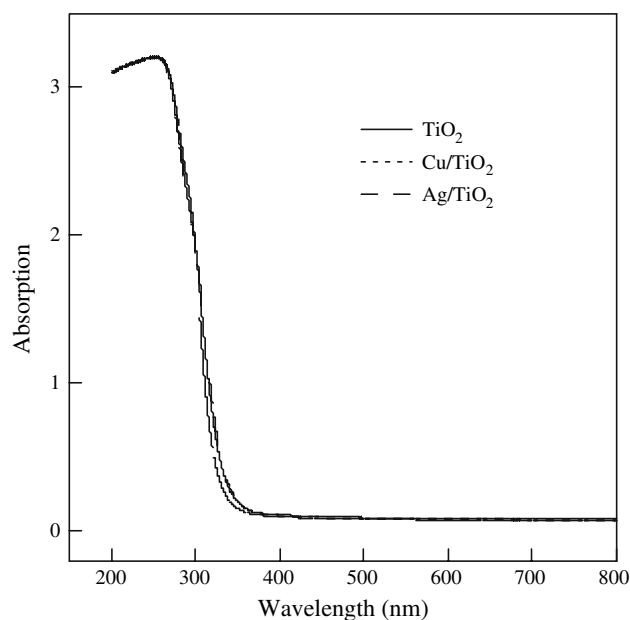**Fig. 4** Schematics of reactor system
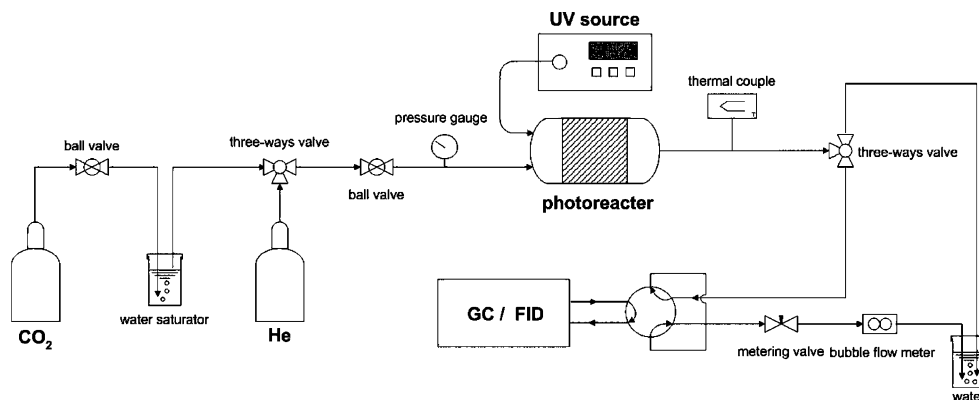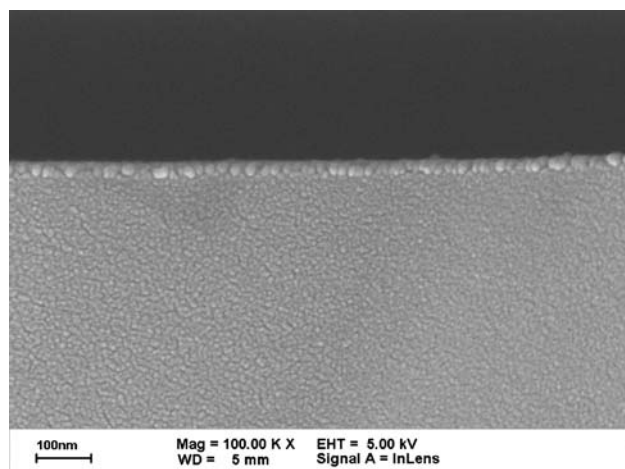
(a) TiO$_2$ film
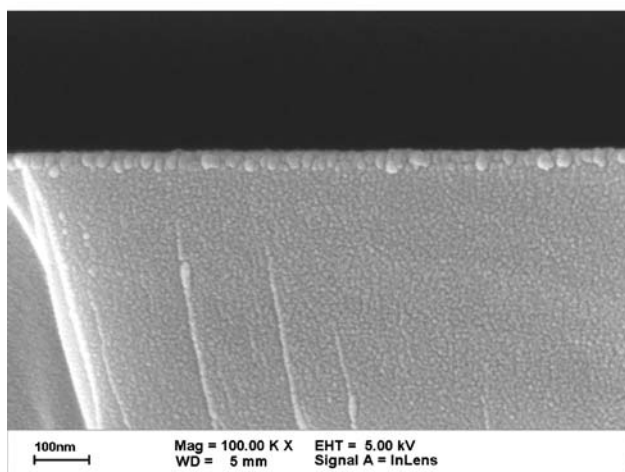
(b) Cu/TiO$_2$ film
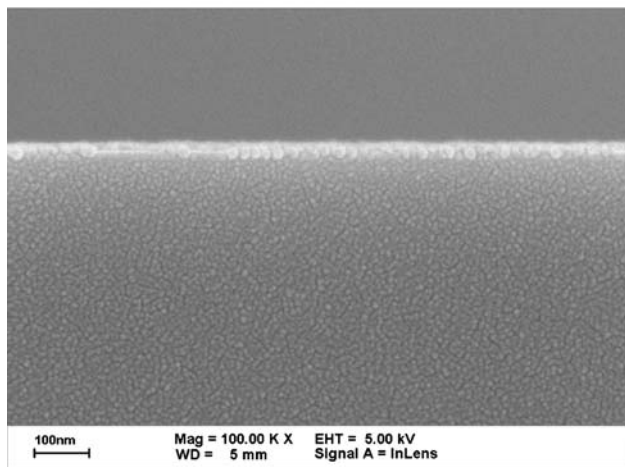
(c) Ag/TiO$_2$ film

Fig. 5 SEM cross sections of TiO$_2$, Cu/TiO$_2$ and Ag/TiO$_2$ films on optical fibers

The XRD spectra in Fig. 6 shows the diffraction patterns of TiO$_2$, Cu/TiO$_2$ and Ag/TiO$_2$ films. Thermal treatment at 500 °C for 5 h results in well crystallized anatase-type

Fig. 6 XRD of TiO$_2$, Cu/TiO$_2$ and Ag/TiO$_2$

Fig. 7 UV spectra of TiO$_2$, Cu/TiO$_2$ and Ag/TiO$_2$

TiO$_2$. No other diffraction peak is observed in the XRD spectra indicating that metal (Cu or Ag) oxide is finely dispersed on TiO$_2$. Figure 7 shows the UV–visible absorption spectra of films. The TiO$_2$ films absorbs light below a wavelength of 380 nm in the UV–Vis spectra. The UV–visible absorptions of Cu/TiO$_2$ and Ag/TiO$_2$ catalysts are similar to those of pure titania.

Table 1 summaries the characteristics of films included crystalline sizes, band gaps and specific surface area. The average crystalline sizes of all films ranged from

Table 1 Characteristics of TiO_2, Cu/TiO_2, Ag/TiO_2 films

Film	Crystal size[a] (nm)	Band gap[b] (eV)	Specific area[c] (m^2/g)
Pure TiO_2	14.4	3.6	59.75
1.2%-Cu/TiO_2	16.8	3.6	55.82
1.0%-Ag/TiO_2	12.0	3.5	71.66

[a] Calculated from the Scherrer equation according to the peak broadening of XRD spectra (at $2\theta = 25.28°$)

[b] Estimated from the UV–VIS spectra extrapolating the absorption edge of VU–Vis spectrum to the abscissa of zero absorption

[c] Measured by N_2 adsorption on powder samples

14 to 17 nm which are consistent with the SEM observation (Fig. 5). In general, the crystalline size is primarily influenced by calcined temperature only, and metal loading has negligible effect. The band gaps ranged from 3.5 to 3.6 eV indicating that the metal loadings do not affect the band structure of TiO_2.

4.2 Photo Reduction of CO_2

Figure 8 shows the methanol yields versus light intensity under the partial pressures of CO_2 and H_2O at 1.19 and 0.03 bar, respectively, at 75 °C. The yields increase with light intensity in the range of 2 to 10 W/cm^2. Pure TiO_2 catalyst gives the least methanol yield, while metal-loaded TiO_2 catalysts improve the yields. The activity of Cu/TiO_2
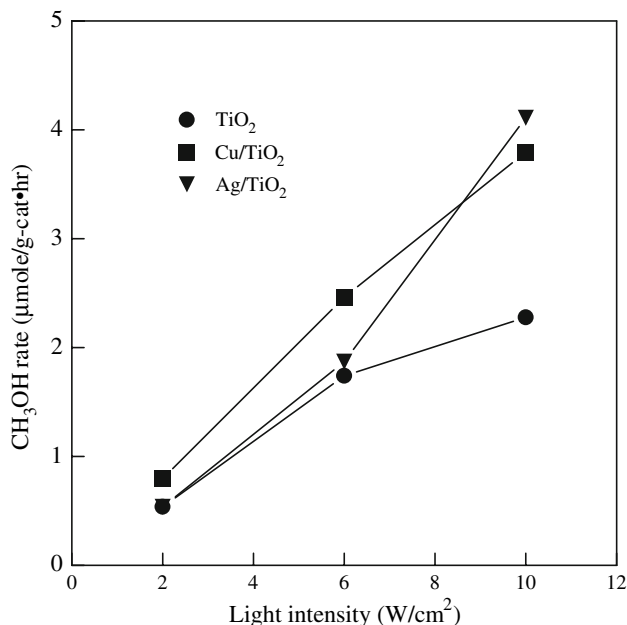
Fig. 8 Methanol yields versus light intensity on TiO_2, Cu/TiO_2 and Ag/TiO_2 (residence time = 5,000 s, P_{CO2} = 1.19 bar, P_{H2O} = 0.03 bar, 75 °C)

Table 2 Apparent quantum efficiency (%) of methanol production on TiO_2, Cu/TiO_2, Ag/TiO_2 catalysts under 365 nm UV irradiation

Light Intensity	TiO_2	1.2% Cu/TiO_2	1.0% Ag/TiO_2
2 W/cm^2	0.00028	0.00033	0.00020
6 W/cm^2	0.00031	0.00035	0.00024
10 W/cm^2	0.00012	0.00013	0.00013

Reaction condition: 75 °C, residence time = 5,000 s, P_{CO2} = 1.19 bar, P_{H2O} = 0.03 bar

Area of Irradiation window: 12.57 cm^2

is slightly higher than that of Ag/TiO_2 when light intensity is lower than 8 W/cm^2. The maximum yield of methanol reaches 4.12 μmole/g-cat h using 1.0 wt% Ag/TiO_2 catalyst under a light intensity of 10 W/cm^2.

Quantum efficiency is an essential factor to evaluate a photo-excited reaction, especially in solar energy utilization. Equation 2 is proposed to determine the overall apparent quantum efficiency. Six moles of electrons are required to produce one mole of methanol from CO_2 (Eq. 1). A pair of electron-hole is assumed to be generated by one photon. The total moles of photon flux are calculated from the UV light intensity and the irradiation area of the OFPR side window.

$$\text{Quantum efficiency (\%)} = \frac{6 \times \text{moles of methanol yield}}{\text{moles of photon flux input}} \times 100\%$$

(2)

Table 2 summaries the apparent quantum efficiency of three catalysts under our experimental conditions. The apparent quantum efficiency represents the effectiveness of photon (UV light) to chemical energy (methanol) conversion. The apparent quantum efficiencies of Cu/TiO_2 and Ag/TiO_2 are slightly higher than those of TiO_2. Either Cu or Ag is an electron trapper and a catalytically active site so that the CO_2 photo reduction can be enhanced. At low light intensity region, 2–6 W/cm^2, the quantum efficiency is almost at the same level. However, the quantum efficiency decreases significantly at a light intensity of 10 W/cm^2. The photon absorption on the TiO_2 may be saturated, thus input photons are over supplied, when UV irradiation is higher than near 8 W/cm^2 under our experimental condition. That is, light energy could be wasted if photon flux is higher than the absorption capacity of a photocatalyst.

The heterogeneous photo reduction of CO_2 involves two procedures, photo activation and catalytic reaction on the catalyst. The factors of photo activation include (1) the excitation of electron-hole pair by photon may not be efficient. Most of photon convert to thermal energy and is dissipated; (2) the recombination of electron and hole could be substantial; and (3) the effective electrons for the catalytic reduction of CO_2 may be only a small portion of total electrons due to migration loss. The factors of catalytic

include (1) the adsorption of CO_2 may be limited on catalyst surface; (2) one of the elementary reaction steps is rate-limiting; and (3) reverse reaction may be occurred. Considering the above factors together, therefore, the overall apparent quantum efficiency can be very low in the CO_2 photo reduction.

5 Summary

An optical-fiber photoreactor is designed and applied to the photo reduction of CO_2 with H_2O using TiO_2, Cu/TiO_2 and Ag/TiO_2-coated optical fibers. The photo reduction of CO_2 is one of the best routes to renewable energy similar to photosynthesis. So far, the maximum methanol yield was 4.12 μmole/g-cat h under 365 nm UV irradiation. Compared with a traditional packed-bed reactor, an optical-fiber provides a medium to transmit light uniformly throughout a reactor. In addition, a higher processing capacity is possible because the catalyst can disperse on a large external area of optical fibers in a given reactor volume. The advantage of photo-driven reaction is clearly benefited from the un-limited solar energy. A high-efficient photoreactor is the first step toward a commercial-scale application to produce chemicals.

References

1. Vione D, Maurino V, Minero C, Pelizzetti E (2001) Chemosphere 45:903–910
2. Kalena GP, Pradhan P, Banerji A (1999) Tetrahedron 55:3209–3218
3. Akkerman I, Janssen M, Rocha J, Wijffels RH (2002) Int J Hydro Ener 27:1195–1208
4. Matsuoka M, Kitano M, Takeuchi M, Anpo M, Thmoas JM (2005) Top Catal 35:305–309
5. Kudo A (2006) Int J Hydro Ener 31:197–202
6. Karakitsou KE, Verykios XE (1993) J Phys Chem 97:1184–1189
7. Hofstadler K, Bauer R, Novallc S, Heisler G (1994) Environ Sci Technol 28:670
8. Peill NJ, Hoffmann MR (1995) Environ Sci Technol 29:2974
9. Tseng I-H, Chang W-C, Wu JCS (2002) Appl Catal B Environ 37:37–48
10. Wu JCS, Lin H-M, Lai C-L (2005) App Catal A Gen 296:194–200
11. Anpo M, Yamashita H, Ikeue K, Fujii Y, Ichihashi Y, Zhang SG, Park DR, Ehara S, Park SE, Chang JS, Yoo JW (1998) Std Surf Sci Catal 114:177–182
12. Guan G, Kida T, Harada T, Isayama M, Yoshida A (2003) Appl Catal A Gen 249:11–18
13. Pathak P, Meziani MJ, Li Y, Cureton LT, Sun Y-P (2004) Chem Commun 10:1234–1235
14. Chu T, Huang H, Tsai D, Annual Meeting of Physics, Taipei, Taiwan, January 17, 2006